*Rev. Roum. Sci. Techn.– Électrotechn. et Énerg.*
Vol. **65**, *1-2*, pp. 47–52, Bucarest, 2020

***Dedicated to the memory of Academician Gleb Drăgan***

# ANALYSIS AND OPTIMIZATION OF A HIGH FREQUENCY PLANAR TRANSFORMER FOR DC-DC CONVERTER USING FINITE ELEMENT METHOD

AMIR BOGZA[1], DAN FLORICAU[1]

**Key words: Power transformer design, Full bridge, Dc-dc converter, Planar magnetic, Finite element method, Automotive.**

**In this paper a method for analyzing and optimization of a high frequency power transformer is presented. The method is applied on designing of the power transformer for a full bridge dc-dc converter used for power conversion in an automotive application. The dc-dc converters used in automotive applications must ensure stable and reliable operation in extreme operating conditions like wide input/output voltage range and elevated temperatures. Improper design of transformer may lead to poor converter performance and thermal issues which may require additional design iterations. The best approach is to construct a virtual prototype of the transformer. Thus, it can be used to perform simulations and optimizations until the desired performance is reached. This goal can be achieved by using finite element method (FEM).**

## 1. INTRODUCTION

Design of magnetic components becomes by far more challenging than ever before. As the operating frequency and power are pushed to the limits, there is an evident need for new methods for design of high power, high frequency and efficient magnetic components. The analysis of the magnetic components performance by using finite element method (FEM) has been widely adopted by engineers especially in the recent years mainly due to evolution of computers processing speed and software innovations.

This method was successfully used at low frequencies for modeling of high voltage three phase transformers, induction motors and generators [1–4], but also at high frequencies for evaluating the efficiency of wireless power transfer between two coils. This allowed finding the values of $R$, $L$, $C$, $M$ parameters [5] and the analysis of impedance matrix in transformer windings [6, 7]. The FEM was also used to investigate the current balancing in parallel windings and for core losses evaluation [8–13].

In all cases, the FEM proved to be very accurate and provided excellent consistency with the measurements performed on real prototypes. Improper magnetic components design may lead to issues like thermal runaway, low efficiency or even saturation of the magnetic core. This usually happens when the flux density, proximity and the skin effects are not evaluated correctly. It is known that the proximity and skin effect can generate significant power losses and hot spots in transformer structure at high frequencies. If the flux density can be determined analytically with acceptable accuracy, the proximity and skin effects are usually difficult to predict by calculations. One way to analyze in details all these complex effects is the FEM.

In this paper, the FEM is used to analyze the performances of a high frequency planar transformer for a dc-dc converter used in an electrical vehicle (EV). The typical power electrical diagram of an EV is provided in Fig. 1. The role of the dc-dc converter is to supply the low voltage car network and to charge the 12 V battery. The car LV network supplies all sensitive consumers like the engine computer, airbags, braking and lights systems. For this reason, the dc-dc converter must be efficient and extremely reliable.

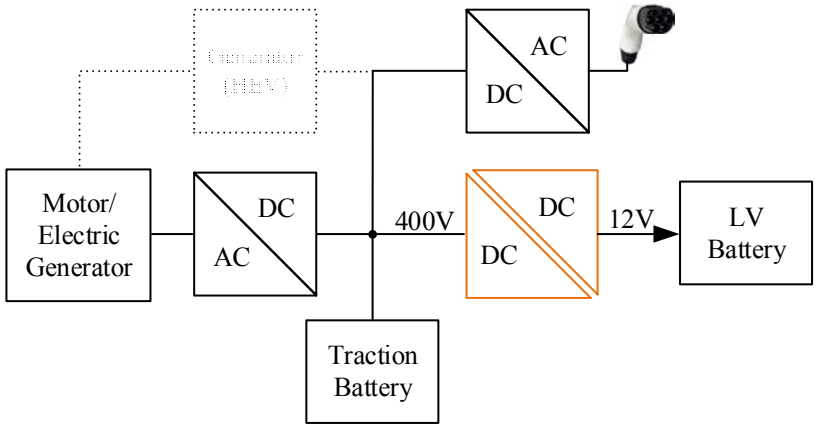


Fig. 1 – The typical power electrical diagram of an EV.

[1] University POLITEHNICA of Bucharest, 313 Splaiul Independenței, 060042 Bucharest, Romania, E-mail: bogzaamir@yahoo.com

The paper is organized as follows. The dc-dc converter and the main waveforms are explained in Section 2. In Section 3, three core types are proposed for the analysis, including the simulation models. The FEM eddy currents and transient simulation results for the proposed core models are presented in Section 4. Finally, conclusions are given.

## 2. THE DC-DC CONVERTER

As mentioned in the previous chapter, the scope of this study is to design and optimize a high frequency planar transformer for a full bridge phase shifted dc-dc converter. In Fig. 2, the electrical diagram of the converter is presented [14].

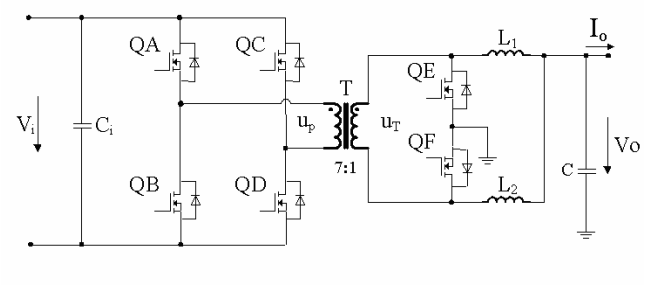


Fig. 2 – Full bridge phase shifted dc-dc converter.

This topology is commonly used for energy conversion [15] from high voltage battery to the 12 V battery and for supplying the low voltage network in hybrid and electric vehicles. The main benefits of the topology are:

- high power density;
- high efficiency due to soft switching;
- galvanic isolation.

In Fig. 3, the main waveforms of the converter are provided [14]. Neglecting the dead time, the operation is the following:

- $[t_0, t_1]$: the voltage $u_T$ is positive due to conduction of QA and QD. QE is turned off and QF is turned on. The transformer secondary current is equal with $i_{L1}$. During this interval, entire load current is passing through QF.
- $[t_1, t_2]$: $u_T$ is zero during this interval due to simultaneous conduction of QA and QC. The QE and QF switches are also in conduction. The $L_2$ current ramp $i_{L2}$ is constant while the current ramp through $L_1$ becomes negative due to negative voltage across $L_1$.
- $[t_2, t_3]$: $u_T$ is negative due to conduction of QC and QB. QE is also turned on, while QF is turned off. The transformer secondary current is equal with $i_{L2}$ current and QE sustains the entire load current.
- $[t_3, t_4]$: $u_T$ is again zero, QB, QD, QE and QF are in conduction. The current ramp $i_{L1}$ remains constant while the current ramp through $L_2$ becomes negative due to negative voltage across $L_1$.

The following specifications of the converter are considered for this analysis:

$P_o$ = 1.65 kW;
$I_o$ = 115 A;
$V_o$ = 12 V÷16 V;
$V_i$ = 240 V ÷ 420 V;
$F_{sw}$ = 200 kHz.

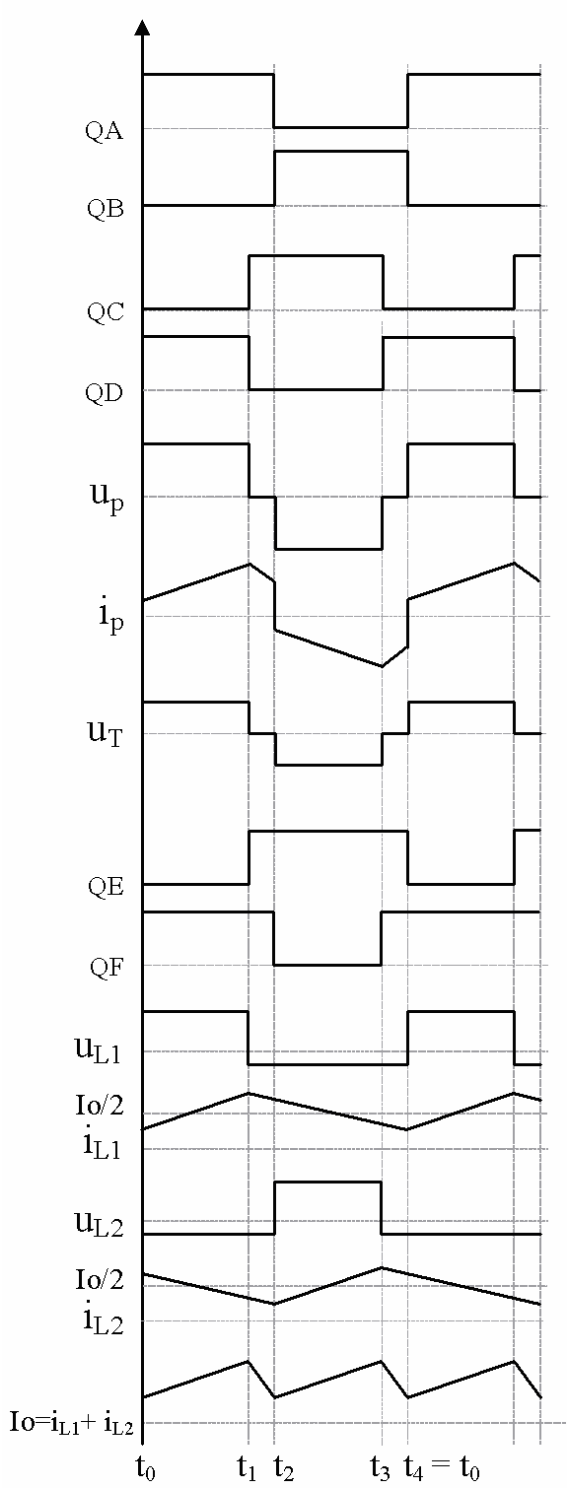


Fig. 3 – Main waveforms of the full bridge phase shifted converter.

## 3. CORE MODELS PROPOSAL

The first step is to choose the transformer core material. Considering that the transformer operates at 200 kHz, a high frequency core material must be selected. For this application, Ferroxcube's 3F3 ferrite material was chosen due to its wide frequency range and low core losses at operating frequency. According to material specifications [16], in order to obtain reasonable core losses at 200 kHz operating frequency, the flux density should be kept less than 150 mT. At this point, the core specific power loss is approximately 0.5 W/cm$^3$.

The next step is to define the model and size of the

magnetic core. The selection of core model and size is very important as it influences the efficiency and power that can be provided by the transformer. Before selecting the core, it is necessary to find the transformer ratio which can be obtained from the transfer function of the converter [14]:

$$V_o = V_{in} \cdot \left( \frac{N_s}{N_p} \right) \cdot D \,. \tag{1}$$

By using the maximum output voltage, the minimum input voltage and the duty cycle ($D$), the ratio of the number of turns of the transformer is obtained:

$$\frac{N_p}{N_s} = \frac{V_{o\max}}{V_{in\min}} \cdot D = 7.5 \,. \tag{2}$$

The transformer ratio it is chosen as the lowest whole number. Therefore, a ratio of seven is used [14].

In order to find the optimum solution, three core models are investigated [17–19]. The cores types were chosen so that two practical implementations could be evaluated. First, a smaller core (E43) with 14 turns in the primary and two turns in the secondary. Second, bigger cores (ER51 and E58) having 7 turns in the primary and one turn in the secondary. The ER51 and E58 have similar cross section. Thus, it is evaluated how the core shape influences the performances of the transformer.

In Table 1, the main datasheet dimensions of the cores are provided.

*Table 1*

Selected core types and dimensions

| Core type | Cross section area | Volume | Bobbin window |
|---|---|---|---|
| E43/10/28 | 229 mm$^2$ | 13.9 cm$^3$ | 13.3 mm |
| ER51/10/38 | 314 mm$^2$ | 25.8 cm$^3$ | 10.9 mm |
| E58/11/38 | 308 mm$^2$ | 24.6 cm$^3$ | 21.1 mm |

In order to perform finite element analysis, the simulation models for the proposed transformers must be first defined. It is considered that all three transformers have the same turns ratio ($N = 7$) and are designed on a six layers printed circuit board (PCB). The configuration of the windings and layers may differ, as the flux density must be limited below 150 mT, to have acceptable core losses.

For this analysis, Ansys Maxwell is used as FEM software tool. The application area of this tool consists in the design and analysis of electric motors, actuators, sensors, transformers and other electromagnetic and electromechanical devices [20].

The main solvers included in Ansys Maxwell are:

- magnetic transient with rigid motion;
- ac electromagnetic;
- magnetostatic;
- electrostatic;
- dc conduction;
- electric transient.

For simulations, an adaptive mesh is used in order to increase the accuracy and to reduce the simulation time. Adaptive mesh means that, in the critical zones where intuitively the magnetic field have a non-uniform distribution (*e.g.* inside and close to air-gaps) the mesh density is high. In the rest, where the magnetic field has a uniform distribution, the mesh density is significantly lower. However, the mesh must be manually or iteratively refined in order to meet the desired energy error limit. For this application, an energy error of 2 % was considered as acceptable.

In Fig. 4, the E43/10/28 transformer simulation model with the windings configuration and associated mesh are presented.

Transformer E43/10/28 has the primary winding of 14 turns distributed in four layers, and two secondary turns placed on the other two layers.

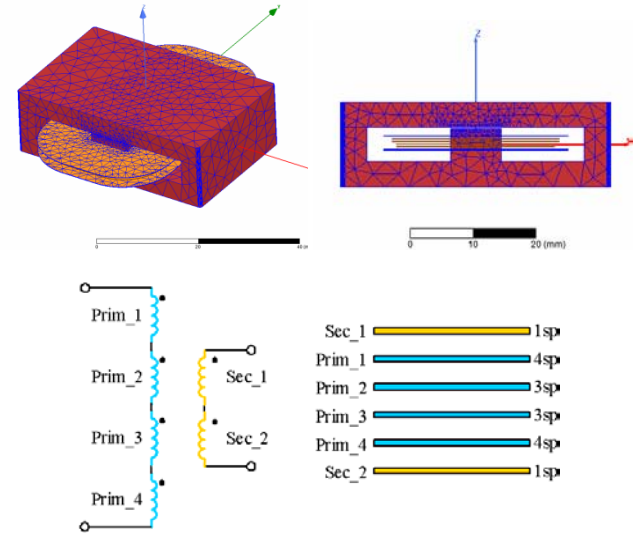


Fig. 4 – Simulation model for E43/10/28 transformer.

The flux density is calculated based input voltage as shown in (3)

$$\hat{B} = \frac{V_{in\max} \cdot D}{2 \cdot S \cdot f_{sw} \cdot N_p} = 85.15 \text{ mT} \,, \tag{3}$$

where

- $V_{\text{inmax}}$ – maximum input voltage;
- $D$ – duty cycle (0.26) for $V_{\text{inmax}}$;
- $S$ – core cross section;
- $f_{\text{sw}}$ – operating frequency;
- $N_{\text{p}}$, – no. of primary turns.

The second simulation model proposed is ER51/10/38 which is presented in Fig. 5. This core model has a small bobbin window, so the number of primary turns must be reduced to seven to avoid excessive copper losses on windings resistance. To maintain the same transformer ratio, four turns are used in parallel for the secondary winding.

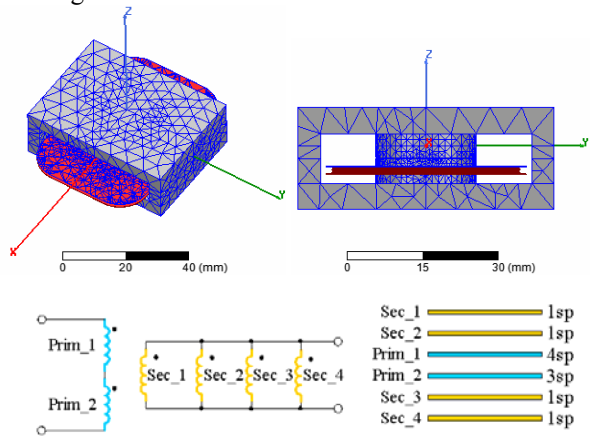


Fig. 5 – Simulation model for ER51/10/38 transformer.

Using (3), the flux density for this configuration reaches 124 mT, significantly higher than E43/10/28 configuration.

The last configuration proposed for evaluation is the E58/11/38 shown in Fig. 6. This core offers much wider bobbin window at similar cross section area with ER51. For this reason, 14 turns are used for the primary winding and two turns in series are used for secondary. As the PCB traces will be larger, the windings resistance should not increase significantly compared to ER51/10/38 configuration. The flux density is 63.3 mT which ensures very low core loss.

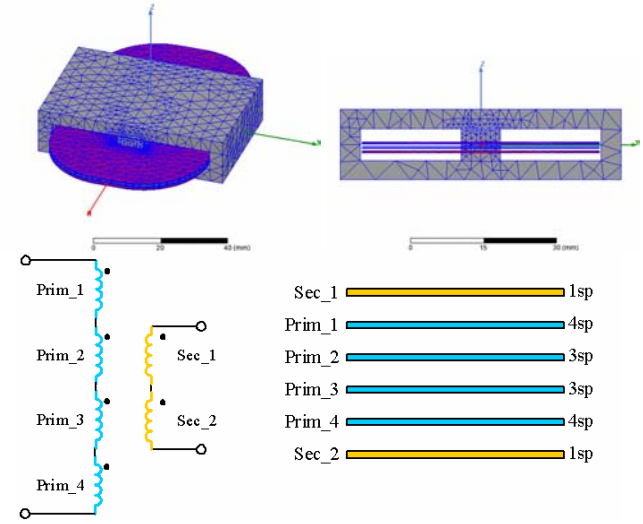


Fig. 6 – Simulation model for E58/11/38 transformer.

## 4. SIMULATION RESULTS

The first FEM simulation introduced is *eddy* currents. This type of simulation assumes sinusoidal voltage and current excitations for the transformer windings. This simulation offers very important information like the windings resistance, magnetizing and leakage inductance, magnetic field distribution and current density. All the data can be plotted across desired frequency range.

The second FEM simulation performed is the *transient* operation, where any current or voltage waveform can be used for the transformer excitation. This type of simulation allows evaluating how the transformer will behave in a real application circuit.

### 4.1. EDDY CURRENTS SIMULATION

The results of the eddy currents simulation of the E58/11/38 transformer are provided in the Fig. 7, where the magnetic field distribution and current density are shown.

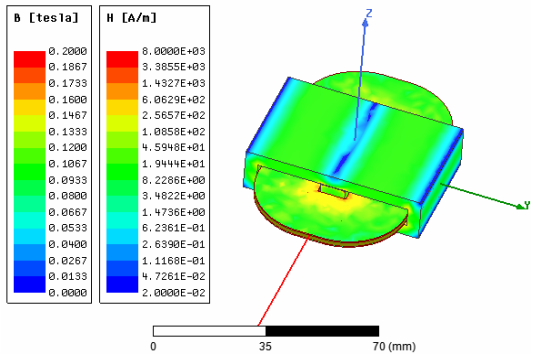


Fig. 7 – Magnetic field distribution and current density in the windings for E58/11/38 transformer.

The main parameters like primary, secondary and leakage inductances (*Lprim*, *Lsec*, *Lleak*) and windings equivalent resistances (*Rprim*, *Rsec*) *versus* switching frequency (*Freq*) are presented in Table 2. The eddy currents simulation results reveal how the windings resistance is affected by the operating frequency. As can be observed, at high frequencies, the skin and proximity effects dominate the winding resistance.

*Table 2*

Inductances and winding resistances for E58/11/38 transformer

| *Freq* | *Lprim* | *Lsec* | *Lleak* | *Rprim* | *Rsec* |
|---|---|---|---|---|---|
| 1 kHz | 382 µH | 7.79 µH | 0.62 µH | 101.2 mΩ | 1.12 mΩ |
| 10 kHz | 378 µH | 7.71 µH | 0.42 µH | 165.1 mΩ | 2.34 mΩ |
| 100 kHz | 378 µH | 7.71 µH | 0.41 µH | 258.1 mΩ | 4.08 mΩ |
| 200 kHz | 379 µH | 7.72 µH | 0.41 µH | 295.3 mΩ | 4.69 mΩ |

The inductances and windings resistance resulted from eddy currents simulation for all three proposed variants are presented in the Table 3. As can be seen, the E43 transformer has more than three times windings resistance, compared to other two core models. This means that copper losses will be also much higher compared to other configurations.

The windings resistances of the ER51 are smaller compared to E58 configuration because it has half of the number of turns of the E58. As the core size is similar, the flux density in the ER51 core is twice the one in E58 leading to significantly higher core loses. Therefore, by using only eddy current simulation, the overall performance of the proposed cores cannot be predicted. In order to find the optimal configuration, a FEM transient simulation is performed.

*Table 3*

Inductances and resistances for transformer configurations at 200 kHz

| Core type | *Lprim* | *Lsec* | *Leak* | *Rprim* | *Rsec* |
|---|---|---|---|---|---|
| E43/10/28 | 279 µH | 5.69 µH | 0.71 µH | 1011 mΩ | 21.51 mΩ |
| ER51/10/38 | 92 µH | 1.87 µH | 0.13 µH | 135 mΩ | 1.72 mΩ |
| E58/11/38 | 379 µH | 7.72 µH | 0.41 µH | 295 mΩ | 4.69 mΩ |

### 4.2. TRANSIENT SIMULATION

The FEM transient simulation in Ansys Maxwell offers the possibility to use external excitations for transformer windings. Therefore, the power schematic of the dc-dc converter is used to simulate the operation of transformer as in the desired application. In this way, the performance can be more accurately evaluated and optimum configuration becomes evident. In Fig. 8, the FEM transient excitation circuit in Ansys Maxwell is presented.

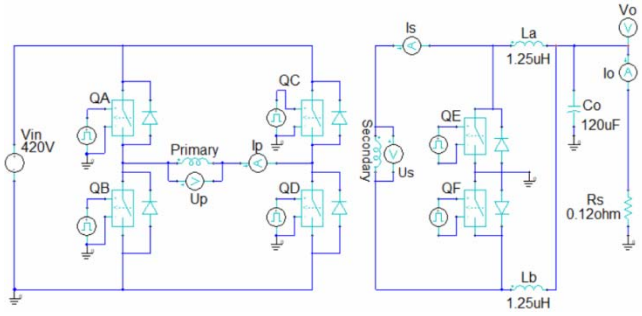


Fig. 8 – FEM transient excitation schematic in Ansys Maxwell.

In Fig. 9, the main transient simulation results for E58/11/38 transformer used in a full bridge phase shifted dc-dc converter are presented. It is noted that main converter waveforms and transformer loss are plotted against time.

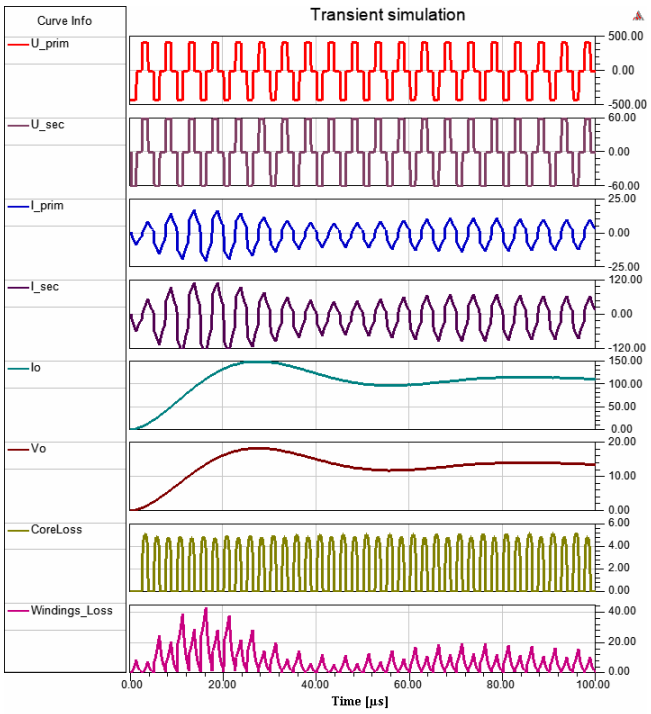


Fig. 9 – Transient simulation results for E58/11/38 transformer operating in a full bridge phase shifted dc-dc converter.

Due to starting the converter with initial conditions of 0 V for all sources and circuit nodes, the instantaneous currents and losses are higher at the beginning where the output capacitors are charged. After performing the simulations for all three transformer variants, a summary of the losses is obtained in Table 4. According to simulation results, the E43 configuration have the highest total power losses and is far from the optimum solution. The ER51 configuration has the lowest windings losses but the highest core losses.

*Table 4*

Power loses breakdown

| Core type | Pwindings | Pcore | Total | Efficiency |
|---|---|---|---|---|
| E43/10/28 | 17.05 W | 2.24 W | 19.29 W | 0.9874 |
| ER51/10/38 | 4.81 W | 8.24 W | 13.05 W | 0.9919 |
| E58/11/38 | 5.97 W | 2.01W | 7.97 W | 0.9950 |

The E58 transformer has higher winding losses than ER51 but significantly lower core losses. The losses in the windings are higher because the number of turns in series for primary and secondary is doubled. In the same time, the core losses are significantly reduced due to the fact the magnetic flux density is halved.

After analyzing the simulation results, the E58/11/38 configuration proved to be the optimum transformer core for the application. The ER51 could be also used if there is not enough space available for E58 and the total losses are under desired specification. Also, adequate cooling must be ensured to avoid core overheating due to operation at higher flux density. The E43 cannot be used for this application due to excessive power losses in the windings that could lead to thermal issues at full load operation.

The finite element simulation offers also the possibility to trace the instantaneous power losses by transformer elements as is illustrated in the Fig. 10. It is noted that power losses are averaged over a few switching cycles after converter is stabilized. In the case of E58 configuration, a good balance between windings and core losses is obtained.

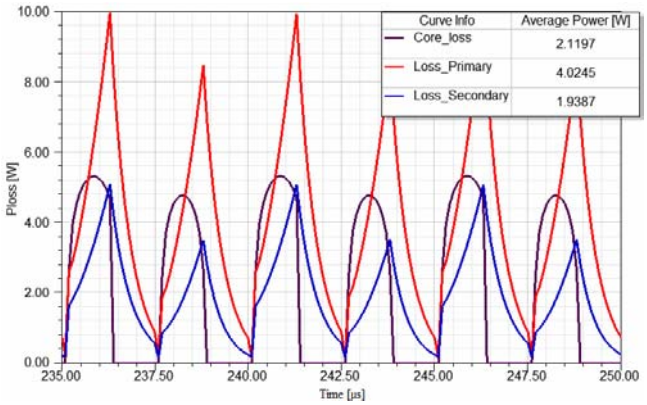


Fig. 10 – E58 power losses distribution

In order to check for any hot spots in transformer windings, a more detailed inspection is realized by tracing the power losses on each PCB layer.

The windings power losses distribution over PCB layers together with transformer primary voltage (*U_prim*) are provided in Fig. 11.

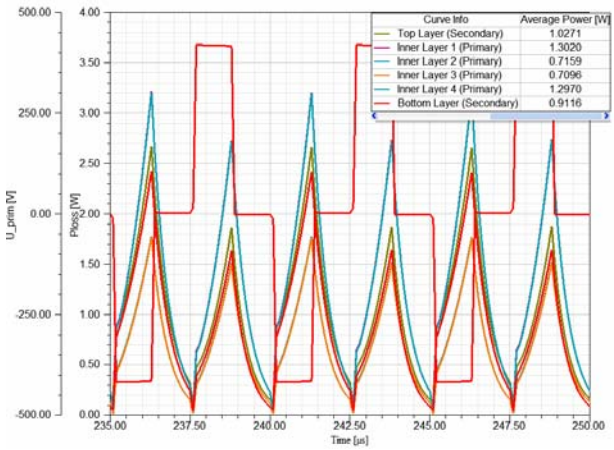


Fig. 11 – E58 power losses distribution by PCB layer.

The results show that are no hot spots in the transformer windings and there is a relatively uniform power loss distribution among PCB layers.

## 5. **CONCLUSIONS**

In this paper a method for analyzing and optimizing of a high frequency planar transformer has been presented. The main objective was to realize a virtual prototype of the transformer and to perform coupled simulations (FEM with Spice circuit) in order to find the best core model and a windings configuration that have the lowest losses.

Thus, two types of finite element analysis ("eddy currents" and "transient") were performed for all three proposed transformer variants.

The best configuration has been found to be E58/11/38, which has total losses, core and windings, close to 8 W, which is less than 0.5 % of the rated power of the dc-dc converter considered in this application.

*Received on December 18, 2019*

## REFERENCES


1. D. Constantin, P. Nicolae, Cristina Nitu, *3D Finite Element Analysis of a Three Phase Power*, IEEE Transactions, Eurocon 2013 conf., pp. 1548–1551, Zagreb, Croatia, July 2013.
2. D. Marcsa, M. Kuczmann, *Two-dimensional modeling of the motion in induction motor with ferromagnetic hysteresis*, Rev. Roum. Sci. Techn. – Électrotechn. et Énerg, **55**, *4*, pp. 351–356 (2010).
3. C. Gheorghe, L. Melcescu, T. Tudorache, E. Mihai, *Numerical modeling approaches for the analysis of squirrel-cage induction motor*, Rev. Roum. Sci. Techn.–Électrotechn. et Energ, **61**, *1*, pp. 18–21 (2016).
4. T. Tudorache, I. Trifu, *Finite element analysis of an axial flux hybrid Wind Generator*, Rev. Roum. Sci. Techn.–Électrotechn. et Energ, **62**, *3*, pp. 229–232 (2016).
5. G. Razmerita, Lavinia Bobaru, Marilena Stanculescu, M. Iordache, D. Niculae, *A Self and Mutual Inductance Calculator*, The 7th International Conference on Modern Power Systems, pp. 2–4, Cluj-Napoca, Romania, June, 2017.
6. D. Alvarez, J. Rosero, E. Mobello, *Analysis of Impedance Matrix in Transformer Windings*, PES Transmission & Distribution Conference and Exposition - Latin America, pp. 1–5, Colombia, September, 2014.
7. A. Reatti, K. Kazimierczuk, *Comparison of various methods for calculating the AC resistance of inductors*, IEEE Transactions on Magnetics, **38**, *3*, pp. 1512 – 1518 (2002).
8. X. Margueron, J.-P. Keradec, A. Besr, *Current Sharing Between Parallel Turns of a Planar Transformer: Prediction and Improvement Using a Circuit Simulation Software*, IEEE Industrial Application Society, pp. 3–7, New Orleans, United States, September 2007.
9. R. Prieto, J. A. Oliver, J. A. Cobos, J. Uceda, *1D magnetic component model for planar structures*, Power Electronics Specialists Conference, PESC99, Charleston (SC), **1**, pp. 574–579 (1999).
10. H. Yuequan, G. Junfeng, B. Xinmin, C. Wie, *Problems of paralleling windings for planar transformer and solutions*, Power Electronics Specialists Conference, PESC02, **2**, pp. 597–601, June, 2002.
11. A. Van den Bossche, V. C. Vaichev, G. B. Georgiev, *Measurement and Loss Model of Ferrites with Non-sinusoidal Waveforms*, 35th Power Electronics Specialists Conference, pp. 2–3, Aachen, Germany, 2004.
12. J-P. Keradec, B. Cogitore, F. Blache, *Power transfer in a two winding transformer from 1D propagation to an equivalent circuit*, IEEE Transactions on Magnetics, **32**, *1*, pp. 2–4 (1996).
13. C. R. Sullivan, T. Abdallah, H. Tacca, K. Venkatachalam, *Accurate Prediction of Ferrite Core Loss with Nonsinusoidal Waveforms using only Steinmetz parameters*, Workshop on Computers in Power Electronics, pp. 1–2, June 2002.
14. A. Bogza, D. Floricau, L. Parvulescu, *Selection of the Power Components for a Phase-Shifted Full-Bridge Converter with Current Doubler,* pp. 1–3, ICATE, Craiova, 2018.
15. M. O'Loughlin, *UCC28950 600-W Phase-Shifted Full-Bridge Application*, Report SLUA560B, pp. 3–14, October 2010.
16. Ferroxcube, *3F3 Material specification*, pp. 2–3, Sept. 2008: https://www.ferroxcube.com/upload/media/product/file/MDS/3f3.pdf.
17. Ferroxcube, *E43/10/29 – Planar E cores*, pp. 2–4, http://ferroxcube.home.pl/prod/assets/e431028.pdf, Sept.2008.
18. Ferroxcube, *ER51/10/38 – Planar E cores*, pp. 2–4, http://ferroxcube.home.pl/prod/assets/er511038.pdf, Sept.2008.
19. Ferroxcube, *E58/11/38 – Planar E cores*, pp. 2–4, http://ferroxcube.home.pl/prod/assets/e581138.pdf, Sept.2008.
20. Ansys, *Ansys Maxwell Product presentation*, pp. 1, https://www.ansys.com/products/electronics/ansys-maxwell, 2020.